ELSEVIER

Chemical Engineering Journal 124 (2006) 89–101

Chemical Engineering Journal

www.elsevier.com/locate/cej

Adsorption kinetics of maxilon blue GRL onto sepiolite from aqueous solutions

Mehmet Doğan [a,*], Mahir Alkan [a], Özkan Demirbaş [a], Yasemin Özdemir [a], Cengiz Özmetin [b]

[a] *Balikesir University, Faculty of Science and Literature, Department of Chemistry, 10100 Balikesir, Turkey*
[b] *Balikesir University, Faculty of Engineering, Department of Environmental Engineering, 10100 Balikesir, Turkey*

Received 11 January 2006; received in revised form 16 July 2006; accepted 6 August 2006

Abstract

Adsorption isotherm of maxilon blue GRL on sepiolite was determined and correlated with common isotherm equations such as Langmuir and Freundlich models. It was found that the Langmuir model appears to fit the isotherm data better than the Freundlich model. Furthermore, adsorption kinetics experiments were carried out to remove the maxilon blue GRL from its aqueous solutions using sepiolite as an adsorbent. The remove rate of maxilon blue GRL by sepiolite was studied by varying parameters such as the contact time, stirring speed, initial dye concentration, ionic strength, pH and temperature. The kinetics experiments indicated that initial dye concentration, ionic strength, pH and temperature could affect the adsorption rate of maxilon blue GRL. Sorption data were fitted to pseudo-first-order, the Elvoich equation, pseudo-second-order, mass transfer and intra-particle diffusion models, and found that adsorption kinetics can be described according to the pseudo-second-order model, from which the rate constant and the adsorption capacity were determined. Rate constants under different conditions were also estimated. In addition, we found that the rate-limiting step was intra-particle diffusion. According to the change of intra-particle diffusion parameter, the adsorption processes could be divided into different stages. Thermodynamic activation parameters such as activation energy E_a, enthalpy ΔH^*, entropy ΔS^* and free energy ΔG^* were determined. These parameters indicate that the adsorption has a low potential barrier corresponding to a physisorption; the adsorption reaction is not a spontaneous one; and the adsorption is physical in nature involving weak forces of attraction and is also endothermic.

Keywords: Sepiolite; Dye; Adsorption; Adsorption isotherms; Adsorption kinetics; Diffusion; Activation parameters

1. Introduction

(Ad)sorption at a solid–liquid interface is a complex process playing a crucial role in numerous industrial applications as well as in the fate and migration of chemical pollutants in the environment. In industry, the sorption techniques employing solid sorbents are widely used to remove certain classes of chemical pollutants from waters, especially those that are hardly destroyed in conventional wastewater treatment plants [1]. Dyes and pigments represent one of the problematic groups because they are toxic in nature with suspected carcinogenic and mutagenic effects [2] that affect aquatic biota and humans [3]. They are emitted into wastewaters from various industrial branches, mainly from the dye manufacturing and textile finishing [4] and also from food coloring, cosmetics, paper and carpet industries. Synthetic dyes have complex aromatic structures which provide them physicochemical, thermal and optical stability [5,6]. The sorption process provides an attractive alternative for the treatment of contaminated waters, especially if the sorbent is inexpensive and does not require an additional pretreatment step (such as activation) before its application [1].

Over the last few decades, adsorption has gained importance as a purification and separation process on an industrial scale and become an attractive option for industrial water treatment, especially the removal of organic compounds that are chemically and biologically stable [7,8]. The first step to an efficient adsorption process is the search for an adsorbent with high selectivity, high capacity, long life and if possible, it has to be available in tonnage quantities and at economical cost. Granular activated carbon is the most popular adsorbent that has been used with great success for the removal of dye from water [9–11]. However, adsorbent-grade activated carbon is cost-prohibitive and

* Corresponding author. Tel.: +90 266 612 10 00; fax: +90 266 612 12 15.
E-mail addresses: mdogan@balikesir.edu.tr (M. Doğan), malkan@balikesir.edu.tr (M. Alkan).

1385-8947/$ – see front matter © 2006 Elsevier B.V. All rights reserved.
doi:10.1016/j.cej.2006.08.016

Nomenclature

C_t	dye concentration in solution at any time t (mol/L)
C_0	initial dye concentration in aqueous solution (mol/L)
D	diffusion coefficient (cm^2/s)
E_a	activation energy (kJ/mol)
ΔG^*	free energy of activation (kJ/mol)
h	Planck's constant
ΔH^*	enthalpy of activation (kJ/mol)
k_b	Boltzmann's constant
k_i	intra-particle diffusion rate constant ($mol/s^{1/2}$ g)
k_0	Arrhenius factor (g/mol s)
k_1	adsorption rate constant for pseudo-first-order kinetic equation ($1\ s^{-1}$)
k_2	adsorption rate constant for pseudo-second-order kinetic equation (g/mol min)
K	adsorption constant (L/mol)
K_F	a constant which is a measure of adsorption capacity (mol/g)
m	mass of adsorbent (g)
m_s	mass of adsorbent per unit volume (g/L)
$1/n$	a measure of adsorption intensity (L/mol)
q_e	equilibrium dye concentration on adsorbent (mol/g)
q_m	the adsorption capacity of adsorbent (mol/g)
q_t	the amount of dye adsorbed per unit mass of the adsorbent at time, t (mol/g)
r_0	the radius of the adsorbent particle (cm)
R_g	gas constant (J/K mol)
R^2	linear regression coefficient
S_s	the surface area of adsorbent (m^2/g)
ΔS^*	entropy of activation (kJ/mol)
t	time (s)
$t_{1/2}$	the half-adsorption time of dye (s)
T	temperature (K)

Greek symbols

α	the initial sorption rate (mol/g min)
β	the desorption constant (g/mol)
β_L	mass transfer coefficient (m/s)

both regeneration and disposal of the used carbon are often very difficult. Therefore, a number of nonconventional sorbents have been tried for the treatment of wastewaters. Natural materials, biosorbents, and waste materials from industry and agriculture represent potentially more economical alternative sorbents. For example, Vijayaraghavan et al. [12] investigated the use of six species of green, brown and red sea weeds as adsorbents. Again, the same authors [13] tested for its ability to remove copper(II) from aqueous solution using a brown marine alga *Turbinaria ornate* as an adsorbent. Moreover, they also reported the pH profiles during both sorption and desorption process.

Sepiolite, ($Mg_4Si_6O_{15}(OH)_26H_2O$), is a natural clay mineral with formula of magnesium hydro-silicate that occurs as a fibrous chain-structure mineral in clays in several areas of the world, although the major commercial deposits of sepiolite are in Spain and Turkey. Its structure, consisting of ribbons alternating with open channels along the fibre axes, has provided sepiolite with good adsorption properties [14,15]. It has been reported that sepiolite has a high adsorptive capacity for many gases and vapours, especially when the dimensions of their molecules allow them to penetrate into the channels of the adsorbent [16,17]. It has been also used as adsorbent of pesticides [18], as a catalyst support [19,20], in the anaerobic digestion of wastewater and solid wastes [21] and also as a support material on the methanogenesis from sewage sludge, reducing the toxic effect of some heavy metals [22]. In the present study, sepiolite has been used as a low-cost adsorbent for the removal of maxilon blue GRL dye. The effects of various factors such as contact time, stirring speed, initial dye concentration, ionic strength, pH and temperature on the adsorption rate of maxilon blue GRL dye on sepiolite from aqueous solutions were investigated. The experimental data was analyzed using various kinetic models such as pseudo-first-order, the Elvoich equation, pseudo-second-order, mass transfer and intra-particle transfer models. In addition, diffusion coefficient and thermodynamic activation parameters for removal of maxilon blue GRL on sepiolite from aqueous solutions were also determined.

2. Materials and methods

2.1. Materials

Sepiolite sample used in this study was obtained from Aktaş Lületaşı Co. (Eskişehir, Turkey). Some physical and physicochemical properties, and the chemical composition of the sepiolite found in Eskişehir, Turkey are given in Tables 1 and 2.

Table 1
Some physical and physicochemical properties of sepiolite

Parameters	Value	References
Surface area ($m^2\ g^{-1}$)	342	[23]
Density ($g\ cm^{-3}$)	2.5	[23]
Cation exchange capacity ($mg\ 100\ g^{-1}$)	25	[23]
pH of solution	7.8–8.3	[23]
Porosity	50.8%	[24]
Color	White	[23]
Melting temperature	1400–1450 °C	[23]
Drying temperature	40 °C	[23]
Reflective index	1.5	[23]

Table 2
The chemical composition of sepiolite [20]

Compounds	Weight (%)
SiO_2	53.47
MgO	23.55
CaO	0.71
Al_2O_3	0.19
Fe_2O_3	0.16
NiO	0.43
Weight losing	21.49

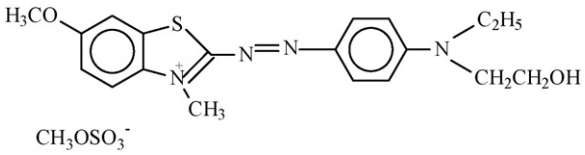

Fig. 1. The structure of maxilon blue GRL.

Maxilon blue GRL [C.I. Basic blue 41, chemical formula: $C_{19}H_{26}N_3O_6S_2$, MW: 456 g/mol, $\lambda_{max} = 608$ nm] was obtained from Setaş Textile Co. (Bursa, Turkey). The structural form of dye is given in Fig. 1. Concentrations of dye were determined by finding out the absorbance at the characteristic wavelength using a double beam UV/Vis spectrophotometer (Cary 1E UV–Visible spectrophotometer, Varian). Calibration curves were plotted between absorbance and concentration of the dye solution.

2.2. Purification of sepiolite

Sepiolite sample was treated before using in the experiments as follows [25,26]: the suspension containing 10 g/L sepiolite was mechanically stirred for 24 h, after waiting for about 2 min the supernatant suspension was filtered through filter paper. The solid sample was dried at 105 °C for 24 h, ground then sieved by 100 μm sieve. The particle sizes in the range of 0–100 μm was used in further experiments.

2.3. Experimental procedure

Studies of the adsorption kinetics of maxilon blue GRL onto sepiolite were carried out from its aqueous solution. The dye solution was prepared with distilled water. In adsorption experiments, the initial dye concentration was 2.0×10^{-3} mol/L, except those in which the effect of dye concentration was investigated. Kinetic experiments were carried out by agitating 2 L of dye solution of known initial dye concentration 2.0×10^{-3} mol/L with 5 g of sepiolite at room temperature (25 °C), pH of 9, 1×10^{-3} mol/L constant NaCl ionic strength and a constant agitation speed of 400 rpm. Fig. 2 shows the schematic diagram of the batch adsorber. Preliminary experiments had shown that the effect of the separation time on the adsorbed amount of dye was negligible. The pH of the solution was adjusted with NaOH or HNO_3 solution by using a Orion 920A pH-meter with a combined pH electrode. pH-meter was standardized with NBS buffers before every measurement. A constant temperature bath was used to keep the temperature constant. A preliminary experiment revealed that about 180 min is required for the adsorption process to reach the equilibrium concentration. The particle was thoroughly mixed with 2 L dye solution in the reaction vessel at constant temperature (25 °C). Two milliliter samples were drawn at suitable time intervals, and were then centrifuged for 15 min at 5000 rpm and the concentration in the supernatant solution was analyzed using a UV–Visible spectrophotometer. Each experimental run continued until no significant change in the dye concentration was measured [27].

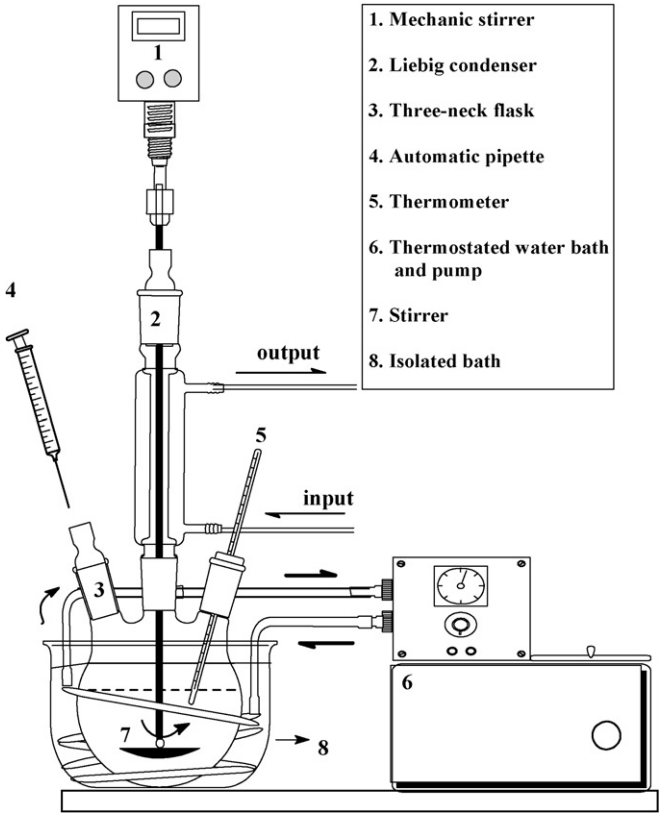

Fig. 2. Schematic diagram of the batch adsorber.

2.4. Calculation

The adsorbed amount of dye at any time t, q_t, was calculated from the mass balance equation:

$$q_t = (C_0 - C_t)\frac{V}{m} \quad (1)$$

where C_0 and C_t are the initial and liquid-phase concentrations at any time t of dye solution (mol/L), respectively, q_t the dye concentration on adsorbent at any time t (mol/g), V the volume of dye solution (L), and m is the mass of sepiolite sample used (g) [23].

3. Results and discussion

3.1. Adsorption isotherm and equilibrium

The adsorption isotherm indicates how the adsorbate molecules distribute between the liquid phase and the solid phase when the adsorption process reaches an equilibrium state. The analysis of the isotherm data by fitting them to different isotherm models is an important step to find the suitable model that can be used for design purposes [28]. Fig. 3 shows a plot of the dye loading on the adsorbent against the dye equilibrium concentration in the liquid phase for maxilon blue GRL at 25 °C. As the initial dye concentration increase, the adsorbed amount of dye on sepiolite increased until equilibrium state.

The analysis and design of adsorption process requires equilibrium to better understand the adsorption process. Sorption

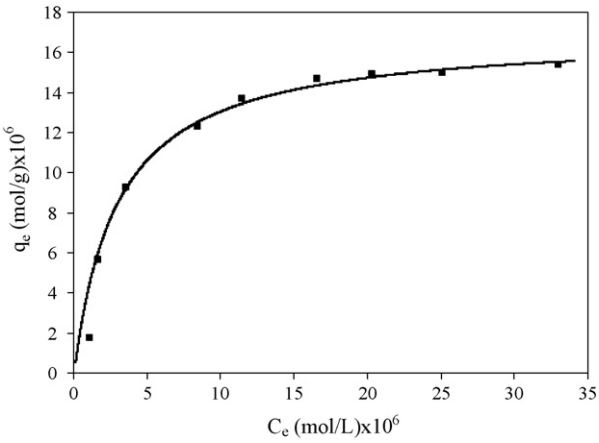

Fig. 3. The best-fit curve obtained according to Langmuir isotherm for adsorption of maxilon blue GRL on sepiolite.

equilibria provide fundamental physiochemical data for evaluating the applicability of sorption process as an unit operation. In the present investigation the equilibrium data were analyzed using the Freundlich and Langmuir isotherm expression given by Eqs. (2) and (3) [29]:

- Freundlich:

$$q_e = K_F C_e^{1/n} \tag{2}$$

- Langmuir:

$$q_e = \frac{q_m K C_e}{1 + K C_e} \tag{3}$$

where q_m is the maximum amount of adsorption (mol/g), K the affinity constant (L/mol), C_e the solution concentration at equilibrium (mol/L), K_F the constant which is a measure of adsorption capacity (mol/g) and $1/n$ is a measure of adsorption intensity (L/mol). The linearized forms of the Freundlich and Langmuir equations can be written as follows:

$$\ln q_e = \ln K_F + \left(\frac{1}{n}\right) \ln C_e \tag{4}$$

$$\frac{C_e}{q_e} = \frac{1}{q_m K} + \frac{C_e}{q_m} \tag{5}$$

For Freundlich isotherm, the plot of $\ln q_e$ against $\ln C_e$ of Eq. (4) should give a linear relationship, from which n and K_F can be determined from the slope and the intercept, respectively. Langmuir isotherm parameters q_m and K can be obtained by plotting C_e/q_e versus C_e. Fig. 4a and b shows the fitted equilibrium data in Freundlich and Langmuir isotherm expressions, respectively. From this figure, it was observed that the equilibrium data fitted both the Freundlich and Langmuir expressions with a correlation coefficient value of 0.7904 and 0.9992, respectively. But the lower correlation coefficient for the Freundlich isotherm confirms the nonapplicability of this model for the maxilon blue GRL/sepiolite systems. The very much higher correlation coefficient of 0.9992 for the Langmuir isotherm predicts the monolayer coverage of maxilon blue GRL on sepiolite particles.

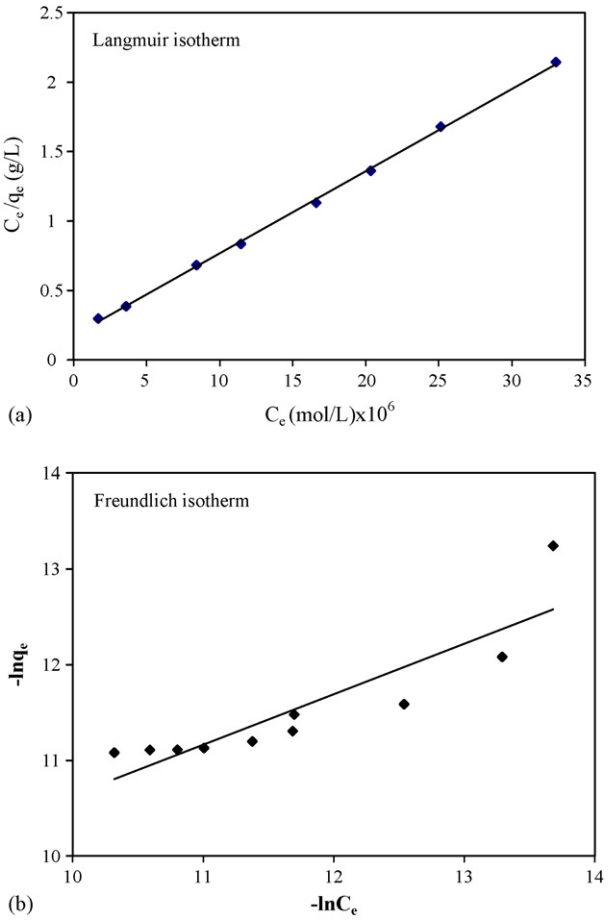

Fig. 4. Langmuir and Freundlich isotherms for Fig. 3.

From Fig. 4, it was calculated that the maximum sorption capacity q_m of sepiolite for maxilon blue GRL was 1.69×10^{-5} mol/g. The Langmuir theory assumes that sorption takes place at specific sites within the adsorbent, which means that once a dye molecule occupies a site, no further adsorption can take place at that site. Therefore, at equilibrium, a saturation point is reached beyond which no further adsorption can occur [30].

3.2. Adsorption rate

The removal rate of maxilon blue GRL on sepiolite was investigated using parameters such as contact time, stirring speed, initial dye concentration, ionic strength, pH and temperature.

3.2.1. Effect of contact time

The necessary contact time to reach the equilibrium depends on the initial dye concentration and the adsorption capacity increases with the initial dye concentration in all cases. Adsorption isotherms are usually determined under equilibrium conditions. A series of contact time experiments for maxilon blue GRL has been carried out with a constant initial dye concentration of 2×10^{-3} mol/L, particle size of 0–100 μm, pH 9, temperature 298 K, constant ionic strength of 1×10^{-3} mol/L NaCl and a constant stirrer speed of 400 rpm. Fig. 5 shows the contact time necessary to reach saturation of dye is about 180 min. As

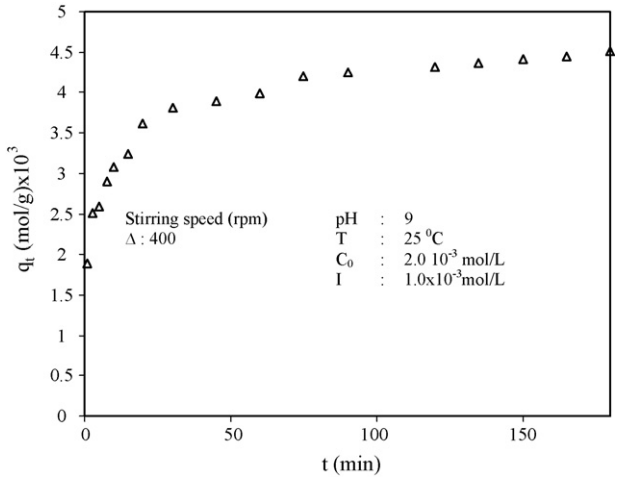

Fig. 5. The effect of contact time to the adsorption rate of maxilon blue GRL on sepiolite.

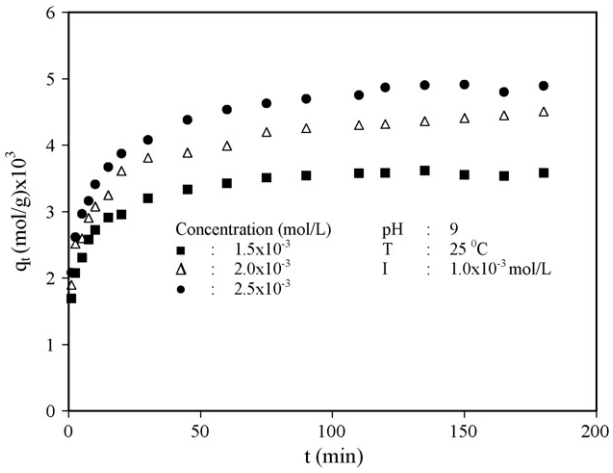

Fig. 7. The effect of initial dye concentration to the adsorption rate of maxilon blue GRL on sepiolite.

seen from Fig. 5, the amount of the adsorbed dye onto sepiolite increases with time and, at some point in time, reaches a constant value beyond which no more is removed from solution. At this point, the adsorbed amount of dye onto sepiolite is in a state of dynamic equilibrium with the amount of the dye desorbing from the adsorbent. The time required to attain this state of equilibrium is termed the equilibrium time, and the adsorbed amount of dye at the equilibrium time reflects the maximum adsorption capacity of the adsorbent under those operating conditions [31].

3.2.2. Effect of stirring speed

The effect of stirring speed on removal rate of maxilon blue GRL with sepiolite at different stirring speeds is shown in Fig. 6. The data shown in Fig. 6 indicates that the difference of adsorption rate was insignificant as the stirring speed increases. Similar phenomena were observed in the kinetic experiments of methyl violet, methylene blue and Victoria blue on perlite [27,32,33] and Basic Brilliant green on modified peat–resin particle [34].

3.2.3. Effect of initial dye concentration

The initial concentration provides an important driving force to overcome all mass transfer resistances of all molecules between the aqueous and solid phases [35–38]. The effect of initial dye concentration on the rate of adsorption is shown in Fig. 7. From Fig. 7, it was observed that the % color removal varied with varying initial maxilon blue GRL concentration, and also observed that at all the initial maxilon blue GRL concentrations, the % color removal was very rapid for the first 30 min and thereafter the sorption rate decreased after 100 min and finally reached saturation after 180 min. Furthermore, larger fractions (80–85%) of total amount of color adsorbed of dye was removed within the first rapid uptake phase, i.e., the first 30 min. This is due to the decrease in flux (concentration gradient) with time due to transfer of solute onto solid phase. The rapid uptake of dye particles at the beginning is due to the occurrence of solute transfer only due to sorbate and sorbent interactions with negligible interference due to solute–solute interactions [39]. Again, the initial rate of adsorption was greater for higher initial dye concentration, because the resistance to the dye uptake decreased as the mass transfer driving force increased.

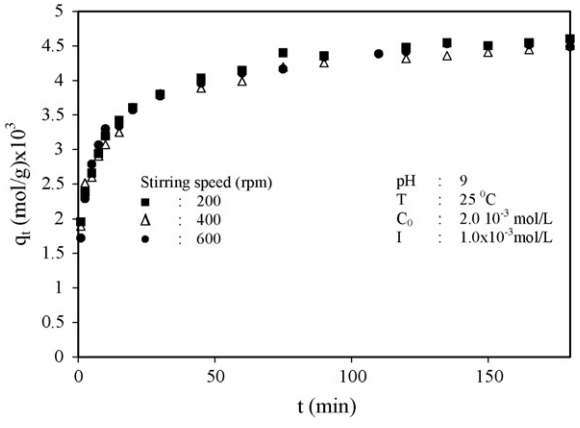

Fig. 6. The effect of stirring speed to the adsorption rate of maxilon blue GRL on sepiolite.

3.2.4. Effect of ionic strength

The effect of inorganic salt (NaCl) on adsorption rate of maxilon blue GRL on sepiolite is presented in Fig. 8. As seen in Fig. 8, the presence of inorganic salt has significantly influenced the adsorption rate of maxilon blue GRL. The dye adsorption increases with the increasing NaCl concentration. This result is different from those reported by Janos et al. [4]. They tested the effect of inorganic salts (NaCl and $CaCl_2$) on some acid and basic dye adsorption and found that the dye adsorption was not affected. But in their investigation, the highest concentration of salts is only 2 mM, which is quite different from this investigation. Our results show that higher concentration of salts promote the adsorption of maxilon blue GRL on sepiolite. The presence of NaCl in the solution may have two opposite effects. On the one hand, since the salt screens the electrostatic interaction of opposite changes of the oxide surface and the dye molecules, the adsorbed amount should decrease with increase of NaCl concentration. On the other hand, the salt causes an increase in the degree of dissociation of the dye molecules by facilitating the

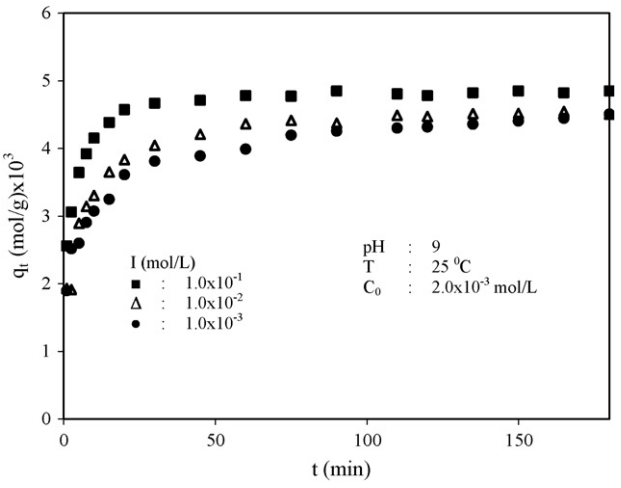

Fig. 8. The effect of ionic strength to the adsorption rate of maxilon blue GRL on sepiolite.

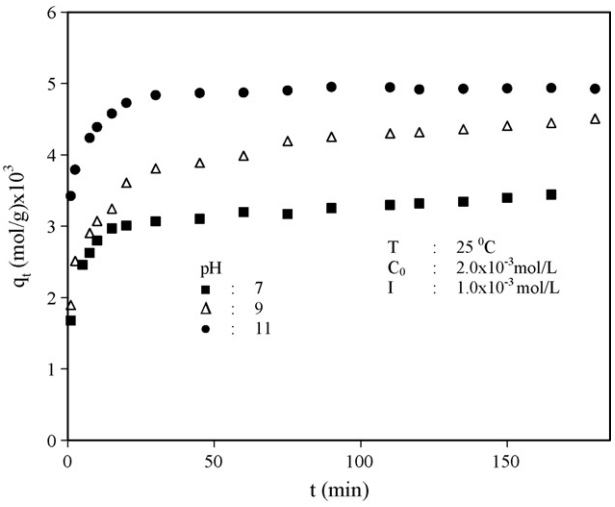

Fig. 9. The effect of initial pH to the adsorption rate of maxilon blue GRL on sepiolite.

protonation. The adsorbed amount increases as the dissociated dye ions free for binding electrostatically onto the solid surface of oppositely changed increase [40–42]. The latter effect seems to be dominant on the adsorption capacity of the surface. For the adsorption of BBF by soils and malachite green by husk-based activated carbon, the adsorption was also found to increase with increasing ionic strength [43,44].

3.2.5. *Effect of pH*

The pH value of the dye solution plays an important role in the whole adsorption process and particularly on the adsorption capacity. Any oxide surface creates a charge (positive or negative) on its surface. This charge is proportional to the pH of the solution, which surrounds the oxide particles. A convenient index of the propensity of a surface to become either positively or negatively charged as a function of pH is the value of the pH required to give zero net surface charge [45]. The variation in the removal rate of maxilon blue GRL with respect to pH can be elucidated by considering the surface charge of the adsorbent materials. The adsorption behavior of maxilon blue GRL on sepiolite was studied in the initial pH range of 7–11. Fig. 9 depicts that the pH significantly affects the extent of adsorption of dye on sepiolite and a increase in the adsorbed amount with increasing pH was observed. The higher adsorption of maxilon blue GRL on sepiolite at high pH may result due to the neutralization of the negative sites at the surface of sepiolite. This facilitates diffusion and provides more of the active surface of the adsorbents resulting thereby enhanced adsorption at their surface. A constant fall in the adsorbed amount with decreasing pH may be due to deprotonation, which hinders the diffusion. We had previously shown that sepiolite had a isoelectrical point at pH 6.6 and exhibited positive zeta potential values at the lower pH values from pH 6.6, and negative zeta potential values at the higher pH values from pH 6.6 [46]. As the pH increases from 7 to 11, the number of ionizable sites on sepiolite increases. In this case:

$$SOH + OH^- = SO^- + H_2O \quad (6)$$

As the pH of the dye solution became higher, the association of dye cations with more negatively charged sepiolite surface could more easily take place:

$$SO^- + Dye^+ = SO^-Dye^+ \quad (7)$$

As the pH of the system increases, the number of positively charged sites decreases and the number of negatively charged sites increases. The negatively charged sites favor the adsorption of dye cations due to electrostatic attraction [47]. A similar effect was previously reported by Mall and Upadhyay [48] for methylene blue adsorption on fly ash particles and Doğan and Alkan [23] for methyl violet adsorption on perlite.

3.2.6. *Effect of temperature*

The temperature has two major effects on the adsorption process. Increasing the temperature is known to increase the rate of diffusion of the adsorbate molecules across the external boundary layer and in the internal pores of the adsorbent particle, owing to the decrease in the viscosity of the solution. In addition, changing the temperature will change the equilibrium capacity of the adsorbent for a particular adsorbate. In this phase of study, a series of experiments were conducted at 5, 15, 25 and 35 °C to study the effect of temperature on the adsorption rate. Fig. 10 depicts the effect of contact time on the rate of adsorption of maxilon blue GRL with sepiolite at four different temperatures. The measurement of kinetics of the process at different temperatures exhibits an increase in the rate of adsorption with the increase in temperature. The result again confirms endothermic nature of the on-going process. However, the half-life of the process decreases with increase in temperature.

3.3. *Adsorption kinetics*

In order to design a fast and effective model, investigations are deliberately made with the kinetic viewpoint. Experimental data obtained was analyzed using following models.

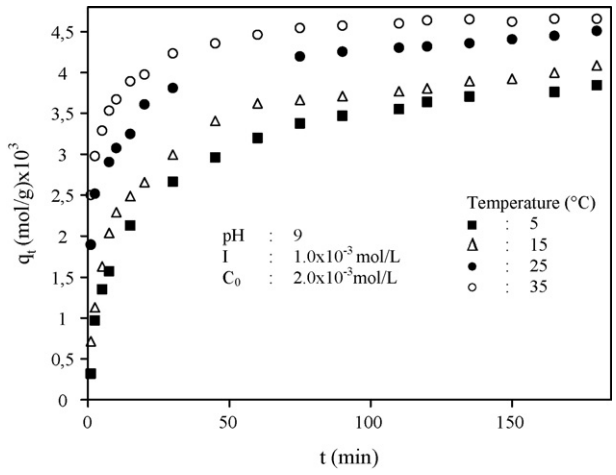

Fig. 10. The effect of temperature to the adsorption rate of maxilon blue GRL on sepiolite.

3.3.1. Pseudo-first-order model

Considering the adsorption behavior of maxilon blue GRL from liquid to solid phase as reversible reaction with equilibrium established in two phases, the specific rate constant for the process was calculated using following Lagergren or pseudo-first-order rate expression [49]. The Lagergren first-order model was given by Eq. (8):

$$\frac{dq_t}{dt} = k_1(q_e - q_t) \tag{8}$$

where k_1 is the rate constant of pseudo-first-order model ($1\ min^{-1}$) and t is the time (min). After definite integration by applying the initial conditions $q_t = 0$ at $t = 0$ and $q_t = q_t$ at $t = t$, the equation becomes [50]:

$$\ln(q_e - q_t) = \ln q_e - k_1 t \tag{9}$$

The plot of $\ln(q_e - q_t)$ versus time (t) gives a straight line and confirms the applicability of the pseudo-first-order rate expression of Lagergren in this case. The equilibrium adsorption capacity, q_e, is required to fit the data, but in many cases q_e remains unknown due to slow adsorption processes. For this reason, it is necessary to obtain the real equilibrium adsorption capacity, q_e, by extrapolating the experimental data to $t = \infty$ or by using a trial and error method. Also, in many cases, the first-order equation of Lagergren does not fit well for the whole range of contact time and is generally applicable over the initial stage of adsorption processes [51–53]. As seen in Table 3, the correlation coefficient values for maxilon blue GRL adsorption on sepiolite have changed in the range of 0.417–0.977. These results have shown that the experimental data do not agree with the pseudo-first-order kinetic model.

3.3.2. The Elvoich equation

In the reactions involving chemical adsorption of adsorbates on solid surfaces without desorption of products, rates may decrease with time due to increasing surface coverage. One of the most useful models of the adsorption process for studies of such activated chemical adsorption is the Elvoich equation [54,55]:

$$\frac{dq_t}{dt} = \alpha \exp(-\beta q_t) \tag{10}$$

where α is the initial sorption rate (mol/g min) and β is the desorption constant (g/mol). To simplify the Elvoich equation, it is assumed that $\alpha\beta t \gg 1$ and by applying the boundary conditions $q_t = 0$ at $t = 0$, this equation becomes

$$q_t = \beta \ln(\alpha\beta) + \beta \ln t \tag{11}$$

Thus, the constants can be obtained from the slope and intercept of a straight line plot of q_t versus $\ln t$. As seen in Table 3, the correlation coefficients for the Elvoich equation have changed in the range of 0.883–0.990. This result has shown that the experimental data do not fit well with the Elvoich equation.

Table 3
Kinetics data calculated for adsorption of maxilon blue GRL on sepiolite

Parameters					Kinetic models							
T (°C)	[C_0] ($\times 10^3$ mol/L)	pH	Stirring speed (rpm)	[I] (mol/L)	First-order or Lagergren	Elvoich equation			Pseudo-second-order			
					R^2	R^2	$\alpha \times 10^{-3}$	$\beta \times 10^4$	q_e (cal.) ($\times 10^4$ mol/g)	q_e (exp.) ($\times 10^4$ mol/g)	k_2 (g/mol min)	R^2
5	2.00	9	400	0.001	0.670	0.975	2.03	6.99	40.30	42.31	1158	0.998
15	2.00	9	400	0.001	0.910	0.987	3.87	6.75	42.50	43.50	1710	0.999
25	2.00	9	400	0.001	0.970	0.984	1.07	4.96	45.38	45.09	2909	0.999
35	2.00	9	400	0.001	0.908	0.972	2.01	3.95	47.19	46.55	4767	0.999
25	1.50	9	400	0.001	0.958	0.962	121.00	1.44	36.40	35.82	5359	0.999
25	2.50	9	400	0.001	0.954	0.987	199.00	2.24	49.93	48.94	2639	0.999
25	2.00	7	400	0.001	0.417	0.990	94.20	2.21	34.20	38.14	2608	0.999
25	2.00	11	400	0.001	0.920	0.995	422.00	1.95	49.61	49.61	13461	0.999
25	2.00	9	200	0.001	0.821	0.987	170.00	2.14	46.50	46.06	2661	0.999
25	2.00	9	600	0.001	0.828	0.988	251.0	2.03	46.08	44.88	2715	0.999
25	2.00	9	400	0.010	0.947	0.944	74.40	5.37	46.14	45.08	3682	0.999
25	2.00	9	400	0.100	0.977	0.883	452.00	4.96	48.79	48.49	8214	0.999

3.3.3. Pseudo-second-order model

The kinetic data were further analyzed using a pseudo-second-order relation proposed by Ho and McKay [39], which is represented by

$$\frac{dq_t}{dt} = k_2(q_e - q_t)^2 \quad (12)$$

where k_2 is the pseudo-second-order rate constant (g/mol min). Separating the variables in Eq. (12) gives

$$\frac{dq_t}{(q_e - q_t)^2} = k_2\, dt \quad (13)$$

Integrating Eq. (13) for the boundary conditions $t = 0$ to $t = t$ and $q_t = 0$ to $q_t = q_t$ gives

$$\frac{t}{q_t} = \frac{1}{k_2 q_e^2} + \frac{t}{q_e} \quad (14)$$

If pseudo-second-order kinetics are applicable, the plot of t/q_t against t for Eq. (14) should give a linear relationship, from which q_e and k_2 can be determined from the slope and the intercept, respectively. Figs. 11–15 show the pseudo-second-order plots for maxilon blue GRL adsorption onto sepiolite for data of Figs. 6–10. The pseudo-second-order rate constant k_2, the calculated q_e value, and the corresponding linear regression correlation coefficient values R^2 are given in Table 3. From Table 3, it was noticed that the linear regression correlation coefficient values, R^2, for second-order model were found to be higher than those of first-order model and the Elvoich equation, and range from 1.0 to 0.998. The higher R^2 values confirm that the sorption data are well represented by pseudo-second-order kinetics

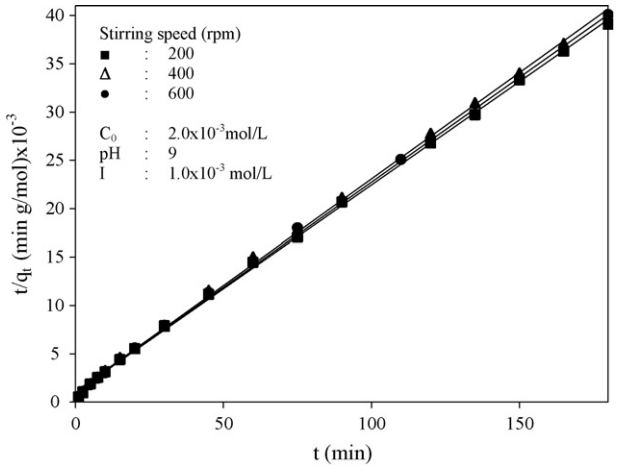

Fig. 11. The plots of t/q_t vs. t for Fig. 6.

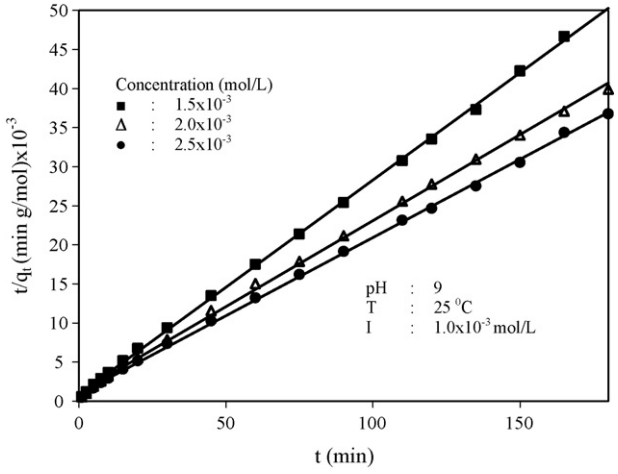

Fig. 12. The plots of t/q_t vs. t for Fig. 7.

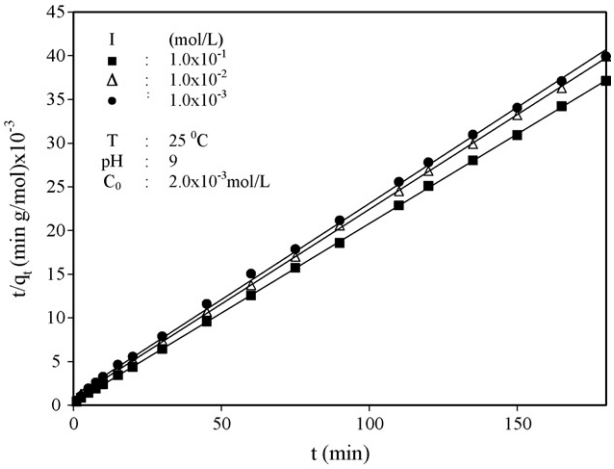

Fig. 13. The plots of t/q_t vs. t for Fig. 8.

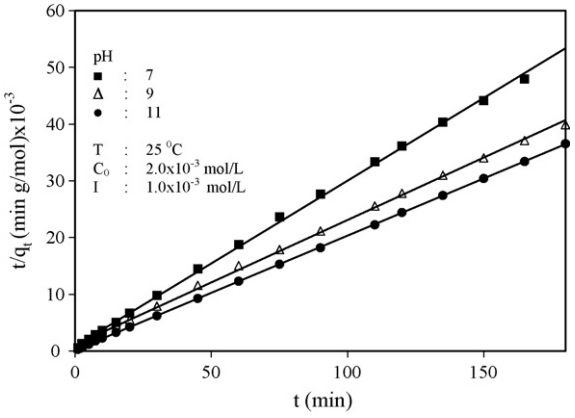

Fig. 14. The plots of t/q_t vs. t for Fig. 9.

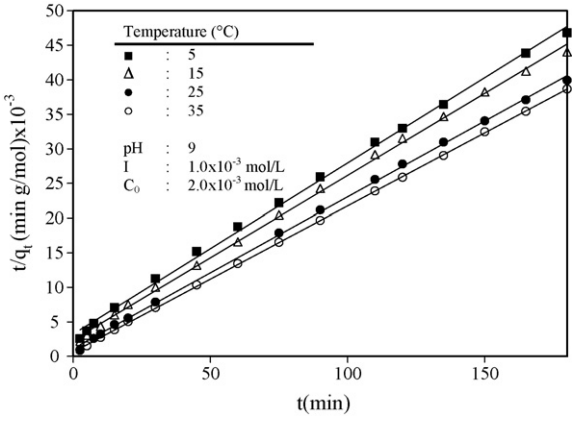

Fig. 15. The plots of t/q_t vs. t for Fig. 10.

Table 4
Adsorption mechanism of maxilon blue GRL on sepiolite

Parameters					Mechanism of adsorption						$t_{1/2}$ (s)
T (°C)	C_0 ($\times 10^3$ mol/L)	pH	Stirring speed (rpm)	[I] (mol/L)	Mass transfer, R^2	Intra-particle diffusion					
						$k_{i,1} \times 10^4$	R_1^2	$k_{i,2} \times 10^5$	R_2^2	D ($\times 10^{10}$ cm^2/s)	
5	2.00	9	400	0.001	0.920	3.30	0.994	6.36	0.996	6.128	345
15	2.00	9	400	0.001	0.916	3.16	0.998	4.66	0.990	7.842	238
25	2.00	9	400	0.001	0.959	3.27	0.992	6.25	0.990	6.270	298
35	2.00	9	400	0.001	0.973	4.47	0.994	7.12	0.994	11.520	162
25	1.50	9	400	0.001	0.970	2.88	0.997	5.10	0.993	9.952	188
25	2.50	9	400	0.001	0.837	4.36	0.992	9.63	0.973	6.694	268
25	2.00	7	400	0.001	0.638	5.42	0.992	4.98	0.992	5.156	362
25	2.00	11	400	0.001	0.884	3.47	0.992	1.36	0.994	30.000	55.0
25	2.00	9	2.00	0.001	0.853	5.54	0.993	1.48	0.982	6.360	294
25	2.00	9	600	0.001	0.907	2.98	0.990	5.98	0.990	6.317	296
25	2.00	9	400	0.010	0.957	7.99	0.995	5.07	0.998	8.615	217
25	2.00	9	400	0.100	0.999	5.56	0.992	7.14	0.988	20.000	91.0

for the entire sorption. The calculated q_e values also agree very well with the experimental data in the case of pseudo-second-order kinetics.

Half-adsorption time, $t_{1/2}$, is defined as the time required for the adsorption to take up half as much sepiolite as its equilibrium value. This time is often used as a measure of the adsorption rate:

$$t_{1/2} = \frac{1}{k_2 q_e} \tag{15}$$

The values of $t_{1/2}$ determined for the tested parameters are given in Table 4.

3.3.4. Adsorption mechanism

From a mechanistic viewpoint, to interpret the experimental data, it is necessary to identify the steps involved during adsorption [56], described by external mass transfer (boundary layer diffusion) and intra-particle diffusion.

3.3.4.1. Mass transfer. Mass transfer coefficient, β_L (m/s) of maxilon blue GRL at the sepiolite–solution interface, were determined by using the Eq. (16) [57]:

$$\ln\left(\frac{C_t}{C_0} - \frac{1}{1+m_s K}\right) = \ln\left(\frac{m_s K}{1+m_s K}\right) - \left(\frac{1+m_s K}{m_s K}\right)\beta_L S_s t \tag{16}$$

where K is the Langmuir constant (L/mol); m_s the mass of adsorbent per unit volume (g/L) and S_s is the surface area of adsorbent (m^2/g). A linear graphical relation between $\ln[(C_t/C_0) - 1/(1+mK)]$ versus t was not obtained. This result indicates that the model mentioned above for the system is not valid. The values of regression coefficient calculated from equation mentioned above are given in Table 4.

3.3.4.2. Intra-particle diffusion model. To interpret the experimental data it is necessary to recognize the steps involved in the process of adsorption that govern the overall rate of removal in each case. For proper interpretation of the kinetic data, the ingenious mathematical treatment recommended by Boyd et al. [58] and Reichenberg [59] has been applied. These mathematical treatments were found to be useful to distinguish between particle diffusion and film diffusion. The adsorption of maxilon GRL onto sepiolite can be divided into three consecutive stages. First, dye migrates through the solution to the exterior surface of sepiolite particle. Second, the dye moves within the particle. Then, third, the dye is adsorbed at sites on the interior surface of sepiolite particle [60]. Many factors can affect the adsorption rate of dye on sepiolite particle, such as the contact time, stirring speed, initial dye concentration, ionic strength, pH and temperature. Generally the third stage is very rapid and does not form a rate-limiting stage in the adsorption. Weber and Morris [61] stated that if intra-particle diffusion is the rate-controlling factor, uptake of the adsorbate varies with the square root of time. Thus, rates of adsorption are usually measured by determining the adsorption capacity of the adsorbent as a function of the square root of time [62]. The mathematical dependence of q_t versus $t^{0.5}$ is obtained if the sorption process is considered to be influenced by diffusion in the spherical particles and convective diffusion in the solution [63,64]. The root time dependence, known also as a Weber–Morris plot [61], may be expressed by the Eq. (17):

$$q_t = k_i \sqrt{t} + C \tag{17}$$

According to Eq. (17), a plot of q_t versus $t^{0.5}$ should be a straight line with a slope k_i and intercept C when adsorption mechanism follows the intra-particle diffusion process. Values of intercept give an idea about the thickness of boundary layer, i.e., the larger the intercept the greater is the boundary layer effect [11]. The intra-particle diffusion plot may represent a multilinearity, representing the different stages in adsorption [34,65,66]. In theory the plot between q_t and $t^{0.5}$ is given by four regions representing the external mass transfer followed by intra-particle diffusion in macro-, meso-, and micropore [39]. The intra-particle diffusion plots for the effect of temperature to the sorption of maxilon blue GRL onto sepiolite were shown in Fig. 16 (other figures

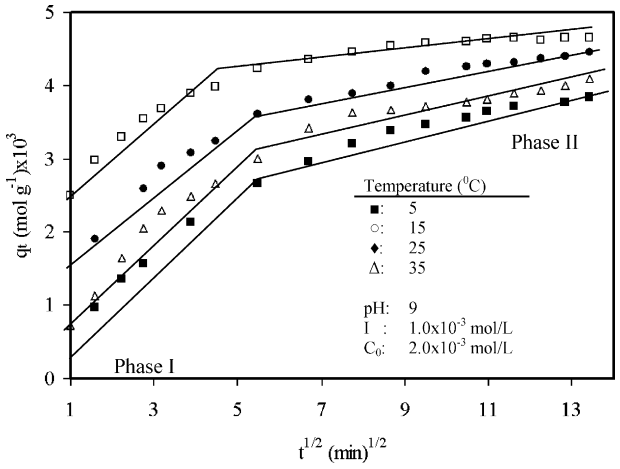

Fig. 16. Intra-particle diffusion plots for different temperatures.

not shown). From this figure, it was observed that there were two linear portions. The double nature of the curve reflects the two-stage external mass transfer followed by intra-particle diffusion of maxilon blue GRL onto sepiolite. The slope of the second linear portion characterizes the rate parameter corresponding to the intra-particle diffusion, whereas the intercept of this second linear portion is proportional to the boundary layer thickness. The intra-particle diffusion constants, $k_{i,1}$ and $k_{i,2}$ (mol/g min$^{0.5}$), is calculated using Eq. (17) from the slope of the corresponding linear region of Fig. 16. The calculated $k_{i,1}$ and $k_{i,2}$ values for different dye conditions are given in Table 4. The $k_{i,1}$ and $k_{i,2}$ express diffusion rates of the different stages in the adsorption. At the beginning, the dye was adsorbed by the exterior surface of sepiolite particle, so the adsorption rate was very fast. When the adsorption of the exterior surface reached saturation, the molecular dye entered into the sepiolite particle by the pore within the particle and was adsorbed by the interior surface of the particle. When the molecular dye diffused in the pore of the particle, the diffusion resistance increased, which caused the diffusion rate to decrease. With decrease of the dye concentration in the solution, the diffusion rate became lower and lower, the diffusion processes reached the final equilibrium stage. Therefore, the changes of $k_{i,1}$ and $k_{i,2}$ could be attributed to the adsorption stages of the exterior surface, interior surface and equilibrium, respectively. On the other hand, Allen et al. [64] thought that there were four separate regions depicting the mass transfer onto peat, i.e., external mass transfer effect, macropore diffusion, transitional pore diffusion and micropore diffusion. Table 5 shows that all of $k_{i,1}$ and $k_{i,2}$ increased with initial dye concentration. The driving force of diffusion was very important for adsorption processes. Generally the driving force changes with the dye concentration in bulk solution. The increases of dye concentration result in increase of the driving force, which will increase the diffusion rate of the molecular dye in pore. Table 5 shows the adsorption orders and mechanisms of some dyes on various adsorbents from aqueous solutions. As seen in Table 5, similar results were found for basic red 22 on pith, for methylene blue on perlite and for methylene blue on fly ash.

3.4. Diffusion coefficient

The values of diffusion coefficient largely depend on the surface properties of adsorbents. The diffusion coefficients for the intra-particle transport of maxilon blue GRL within the pores of sepiolite particles have been calculated under various conditions by employing the Eq. (18) [27]:

$$t_{1/2} = \frac{0.030 r_0^2}{D} \tag{18}$$

where D is the diffusion coefficient with the unit cm^2/s, $t_{1/2}$ the time (s) for half adsorption of maxilon blue GRL and r_0 is the radius of the adsorbent particle in cm. The value of r_0 was calculated as 2.5×10^{-3} cm for sepiolite sample. In these calculations, it has been assumed that the solid phase consists of spherical particles with an average radius between the radii corresponding to upper- and lower-size fractions. Table 5 has shown the diffusion coefficients calculated for adsorption of some dyes on various adsorbents from aqueous solutions. We found that the diffusion coefficients in this study changed in the range of 5.16×10^{-10} to 30×10^{-10} cm^2/s under various conditions using Eq. (18) (Table 4). For example, as seen from Table 6, the values of diffusion coefficients increased from 6.128×10^{-10} to 11.520×10^{-10} cm^2/s with change in temperature from 5 to 35 °C, respectively. Based on Table 6, the new results are comparable to those published in literature.

Table 5
Adsorption order and mechanism of some dyes on various adsorbents

Adsorbents	Reaction order	Adsorbates	Adsorption mechanism	References
Fly ash	Pseudo-second-order	Methylene blue	Particle diffusion	[29]
Biosorbent	Pseudo-first-order	Methylene blue	–	[30]
Bottom ash	Pseudo-first-order	Quinoline yellow	–	[67]
Calcined alunite	Pseudo-second-order	Reactive dyes	Mass transfer	[68]
Bagasse fly ash	Pseudo-second-order	Orange-G, methyl violet	–	[69]
Activated carbon	First order	Methylene blue	Intra-particle diffusion	[11]
Pith	Pseudo-second-order	Basic red 22	Intra-particle diffusion	[39]
Wood	–	Astrazon blue	Intra-particle diffusion	[63]
Perlite	Pseudo-second-order	Methylene blue	Intra-particle diffusion	[32]
Perlite	Pseudo-second-order	Methyl violet	Intra-particle diffusion	[27]
Perlite	Pseudo-second-order	Victoria blue	–	[33]
Modified peat–resin particle	–	Basic dyes	Intra-particle diffusion	[34]

Table 6
Diffusion coefficients of some dyes on various adsorbents

Adsorbents	Adsorbates	Diffusion coefficients, D ($\times 10^{10}$ cm^2/s)	References
Fly ash	Methylene blue	20.6	[29]
Shale oil ash	Reactive dyes	7000–12700	[70]
Carbon	Phenol	901	[71]
Carbon	Benzene	80	[71]
Wood	Astrazone blue	0.006–0.0018	[63]
Wood	Teflon blue	0.003–0.008	[63]
Perlite	Methylene blue	24.2–68.7	[32]
Perlite	Methyl violet	17.4–27.7	[27]
Sepiolite	Maxilon blue GRL	5.16–30.00	In this study

3.5. Activation parameters

Arrhenius equation for second-order kinetics model is given as follows:

$$\ln k_2 = \ln k_0 - \frac{E_a}{R_g T} \tag{19}$$

where E_a is the activation energy (J/mol), k_2 the rate constant of sorption (g/mol s); k_0 the Arrhenius factor, which is the temperature independent factor (g/mol s); R_g the gas constant (J/K mol) and T is the solution temperature (K). The slope of plot of $\ln k_2$ versus $1/T$ is used to evaluate E_a. The magnitude of activation energy gives an idea about the type of adsorption which is mainly physical or chemical. Low activation energies (5–40 kJ/mol) are characteristics for physisorption, while higher activation energies (40–800 kJ/mol) suggest chemisorption [72]. The result obtained is +33.96 kJ/mol for the adsorption of maxilon blue GRL onto sepiolite, indicating that the adsorption has a potential barrier and corresponding to a physisorption (Fig. 17). This value is consistent with the values in the literature where the activation energy was found to be 43.0 kJ/mol for the adsorption of reactive red 189 on cross-linked chitosan beads [73], and 5.6–49.1 kJ/mol for the adsorption of polychlorinated biphenyls on fly ash [72].

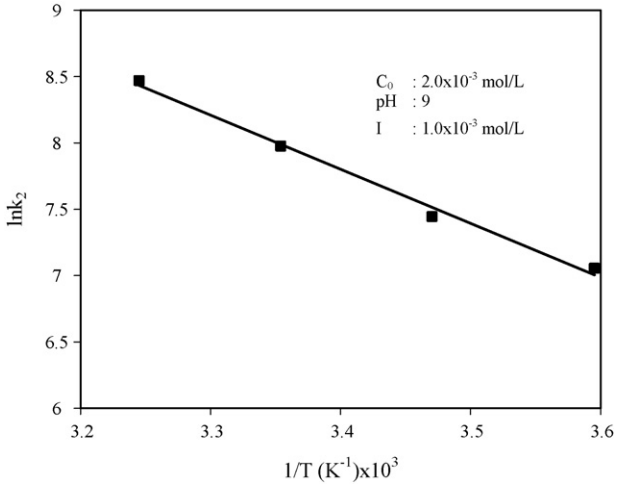

Fig. 17. Arrhenius plot for the adsorption of maxilon blue GRL on sepiolite.

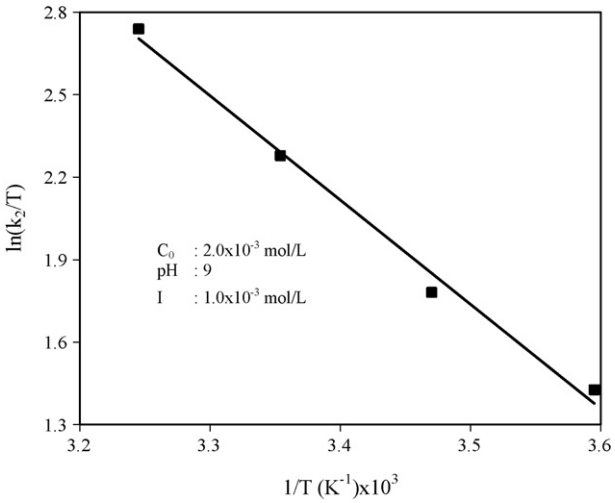

Fig. 18. Plot of $\ln(k_2/T)$ vs. $1/T$ for adsorption of maxilon blue GRL on sepiolite.

The another aim of this paper is to consider the effect of solution temperature on the transport/kinetic process of dye adsorption. Therefore, the thermodynamic activation parameters of the process such as enthalpy ΔH^*, entropy ΔS^* and free energy ΔG^* were determined using the Eyring Eq. (20) [74]:

$$\ln\left(\frac{k_2}{T}\right) = \ln\left(\frac{k_b}{h}\right) + \frac{\Delta S^*}{R_g} - \frac{\Delta H^*}{R_g T} \tag{20}$$

where k_b is the Boltzmann constant (1.3807×10^{-23} J/K) and h is the Planck constant (6.6261×10^{-34} J s). Fig. 18 has shown the plot of $\ln(k_2/T)$ against $1/T$. Generally, the change of free energy for physisorption is between −20 and 0 kJ/mol, but chemisorption is a range of −80 to −400 kJ/mol [75]. The results obtained are +21.85 kJ/mol at 20 °C. This indicated that the adsorption reaction was not a spontaneous one and that the system gained energy from an external source. The value of the standard enthalpy change (31.53 kJ/mol) indicates that the adsorption is physical in nature involving weak forces of attraction and is also endothermic, thereby demonstrating that the process is stable energetically. At the same time, the low value of ΔH^* implies that there was loose bonding between the adsorbate molecules and the adsorbent surface [76]. The negative standard entropy change (ΔS^*) value (−73.2 J/K mol) corresponds to a decrease in the degree of freedom of the adsorbed species.

3.6. Conclusions

In this study, we found that the rate of adsorption of maxilon blue GRL on sepiolite increased by increasing in the initial dye concentration, ionic strength, pH and temperature, but the change of agitation speed did not cause a significant difference of intra-particle diffusion parameter under experimental conditions. The adsorption processes of maxilon blue GRL on sepiolite particle could be well described by intra-particle diffusion model, and the adsorption rate was mainly controlled by the diffusion rate of the molecular dye within a particle. The initial dye concentration could significantly affect the diffusion rate of molecular dye in a particle. The diffusion rate

of dye increased with initial dye concentration. The initial rate of adsorption of maxilon blue GRL with sepiolite was high, and then it declines with time until it reaches a plateau. The adsorption of maxilon blue GRL can easily be described by the two-resistance's model. Langmuir model appeared to fit the isotherm data better than the Freundlich model. The activation energy of adsorption can be evaluated using the pseudo-second-order rate constants. The positive value of E_a (+33.96 kJ/mol) confirms the nature of physisorption of maxilon blue GRL onto sepiolite. The enthalpy change (ΔH^*) for the adsorption process was 31.53 kJ/mol, which did not indicate very strong chemical forces between the dye molecules and sepiolite. The ΔG^* values were positive therefore the adsorption was not spontaneous and the negative value of ΔS^* suggests a decreased randomness at the solid/solution interface and no significant changes occur in the internal structure of the adsorbent through the adsorption of maxilon blue GRL onto sepiolite. The results of this research were compared to the published data in the same field, and found to be in agreement with most of them. The kinetic data may be useful for environmental technologist in designing treatment plants for color removal from wastewaters enriched with maxilon blue GRL. Sepiolite has a high potential to adsorb reactive dyes from aqueous solutions. Therefore, it can be effectively used as an adsorbent for the removal of maxilon blue GRL from wastewaters.

References

[1] P. Janos, V. Smidova, J. Colloid Interf. Sci. 291 (2005) 19–27.
[2] G. McKay, M.S. Otterburn, D.A. Aga, Water Air Soil Pollut. 24 (1985) 307–322.
[3] A.R. Gregory, S. Kanan, P. Kluge, J. Appl. Toxicol. 1 (1991) 308–313.
[4] P. Janos, H. Buchtova, M. Ryznarova, Water Res. 37 (2003) 4938.
[5] G. McKay, S.J. Allen, I.F. Meconney, M.S. Ottrburn, J. Colloid Interf. Sci. 80 (2) (1981) 323–339.
[6] S. Seshadri, P.L. Bishop, A.M. Agha, Waste Manage. 15 (1994) 127–137.
[7] R.P.S. Suri, J. Liu, D. Hand, J.C. Crittenden, D. Perram, J. Air Waste Manage. Assoc. 49 (1999) 951–958.
[8] P. Cyr, R.P.S. Suri, E. Helmig, Water Res. 36 (2002) 4725–4734.
[9] G. McKay, J. Chem. Technol. Biotechnol. 32 (1982) 759–772.
[10] V.K. Gupta, S.K. Srivastava, D. Mohan, Ind. Eng. Chem. Res. 36 (1997) 2207.
[11] N. Kannan, M. Sundaram, Dyes Pigments 51 (2001) 25–40.
[12] K. Vijayaraghavan, J. Jegan, K. Palanivelu, M. Velan, Sep. Purif. Technol. 44 (11) (2005) 53–59.
[13] K. Vijayaraghavan, J. Jegan, K. Palanivelu, M. Velan, Chem. Eng. J. 106 (2) (2005) 177–184.
[14] N. Bektas, B.A. Agim, S. Kara, J. Hazard. Mater. B 112 (2004) 115–122.
[15] S. Calliere, S. Henin, M. Rautureau, Mineralogie des Argiles II. Classification et Nomenclature, 2nd ed., Masson Publisher, 1982.
[16] T. Hibbino, A. Tsunashima, A. Yamazaki, R. Otsuka, Clays Clay Miner. 43 (1995) 391–396.
[17] E. Galan, Clay Miner. 31 (1996) 443–453.
[18] E. Gonzalez-Pradas, M. Villafranca-Sanchez, M. Socias-Viciana, M. Fernandez-Perez, M.D. Urena-Amate, J. Chem. Technol. Biotechnol. 74 (1999) 417–422.
[19] M. Rautureau, C. Tchoubar, Clays Clay Miner. 24 (1976) 42–46.
[20] J.M. Campelo, A. Garcia, F. Lafont, D. Luna, J.M. Marinas, Synth. Commun. 24 (10) (1994) 1345–1350.
[21] C. Maqueda, J.L. Perez-Rodrıguez, L. Lebrato, Fresenius Environ. Bull. 4 (2) (1995) 129–134.
[22] M.A. Munoz, J.C. Codina, A. Devicente, J.M. Sanchez, J.J. Borrego, M.A. Morinigo, Lett. Appl. Microbiol. 23 (5) (1996) 339–342.
[23] M. Alkan, S. Çelikçapa, Ö. Demirbaş, M. Doğan, Dyes Pigments 65 (3) (2005) 251–259.
[24] A.A. Göktaş, Z. Misirli, T. Baykara, Ceram. Int. 23 (1997) 305–311.
[25] M. Alkan, M. Doğan, J. Colloid Interf. Sci. 243 (2001) 280–291.
[26] M. Doğan, M. Alkan, Y. Onganer, Water Air Soil Pollut. 120 (2000) 229–248.
[27] M. Doğan, M. Alkan, Chemosphere 50 (2003) 517–528.
[28] M. El-Guendi, Adsorpt. Sci. Technol. 8 (2) (1991) 217–225.
[29] K.V. Kumar, V. Ramamurthi, S. Sivanesan, J. Colloid Interf. Sci. 284 (2005) 14–21.
[30] E. Rubin, P. Rodriguez, R. Herrero, J. Cremades, I. Barbara, M.E. Sastre de Vicente, J. Chem. Technol. Biotechnol. 80 (2005) 291–298.
[31] K.R. Ramakrishna, T. Viraraghavan, Water Sci. Technol. 36 (1997) 189.
[32] M. Doğan, M. Alkan, A. Türkyılmaz, Y. Özdemir, J. Hazard. Mater. B 109 (2004) 141–148.
[33] M. Alkan, M. Doğan, Fresenius Environ. Bull. 12 (5) (2003) 418–425.
[34] Q. Sun, L. Yang, Water Res. 37 (7) (2003) 1535–1544.
[35] F. Banat, S. Al-Asheh, L. Al-Makhedmeh, Process Biochem. 39 (2003) 193–202.
[36] Y.S. Ho, T.H. Chiang, Y.M. Hsuesh, Process Biochem. 40 (2005) 119–124.
[37] R.S. Juang, F.C. Wu, R.L. Tseng, Environ. Technol. 18 (1997) 525–531.
[38] G. Dönmez, Z. Aksu, Process Biochem. 38 (2002) 751–762.
[39] Y.S. Ho, G. McKay, Can. J. Chem. Eng. 76 (1998) 822.
[40] N. Tekin, O. Demirbaş, M. Alkan, Microporous Mesoporous Mater. 85 (3) (2005) 340–350.
[41] F. Blockhaus, J.M. Sequaris, H.D. Narres, M.J. Schwuger, J. Colloid Interf. Sci. 186 (1997) 234–247.
[42] K. Vermöhlen, H. Lewandowski, H.D. Narres, M.J. Schwuger, Colloids Surf. A 163 (2000) 45–53.
[43] J. German-Heins, M. Flury, Geoderma 97 (2000) 87–101.
[44] Y. Guo, S. Yang, W. Fu, J. Qi, R. Li, Z. Wang, H. Xu, Dyes Pigments 56 (2003) 219–229.
[45] Y. Al-Degs, M.A.M. Khraisheh, S.J. Allend, M.N. Ahmad, Water Res. 34 (2000) 927.
[46] M. Alkan, Ö. Demirbaş, M. Doğan, J. Colloid Interf. Sci. 281 (1) (2005) 240–248.
[47] C. Namasivayam, R. Radhika, S. Suba, Waste Manage. 21 (2001) 381.
[48] I.D. Mall, S.N. Upadhyay, J. Indian Pulp Paper Technol. Assoc. 7 (1) (1995) 51–57.
[49] K. Periasamy, C. Namasvayam, Ind. Eng. Chem. Res. 33 (1994) 317.
[50] S. Lagergren, Ksver Veterskapsakad Handl. 24 (1898) 1–6.
[51] Z. Aksu, S. Tezer, Process Biochem. 36 (2000) 431.
[52] M.S. Chiou, H.-Y. Li, J. Hazard. Mater. 93 (2002) 233.
[53] Y.S. Ho, G. McKay, Process Biochem. 34 (1999) 451.
[54] C. Aharoni, F.C. Tompkins, Kinetics of adsorption and desorption and the Elvoich equation, in: D.D. Eley, H. Pines, P.B. Weisz (Eds.), Advances in Catalysis and Related Subjects, vol. 21, Academic Press, New York, 1970, pp. 1–49.
[55] K. Klusacek, R.R. Hudgins, P.L. Silveston, Chem. Eng. Sci. 44 (1989) 2377–2381.
[56] V.K. Gupta, I. Ali, J. Colloid Interf. Sci. 271 (2004) 321–328.
[57] D. Batabyal, A. Sahu, S.K. Chaudhuri, Sep. Technol. 5 (4) (1995) 179–186.
[58] G.E. Boyd, A.W. Adamson, L.S. Meyers, J. Am. Chem. Soc. 69 (1947) 2836.
[59] D. Reichenberg, J. Am. Chem. Soc. 75 (1953) 589.
[60] C.Y. Chang, W.T. Tsai, C.H. Ing, C.F. Chang, J. Colloid Interf. Sci. 260 (2003) 273–279.
[61] W.J. Weber, J.C. Morris, J. Sanit. Eng. Div. ASCE 89 (SA2) (1963) 31–59.
[62] Y.S. Ho, G. McKay, Process Biochem. 38 (2003) 1047–1061.
[63] G. McKay, V.J.P. Poots, J. Chem. Tech. Biotechnol. 30 (1980) 279–292.
[64] S.J. Allen, G. McKay, K.Y.H. Khader, Environ. Pollut. 56 (1989) 39–50.
[65] K. Vermöhlen, H. Lewandowski, H.D. Narres, M.J. Schwuger, Colloids Surf. A 163 (2000) 45–53.
[66] M. Sankar, G. Sekaran, S. Sadulla, T. Ramasami, J. Chem. Technol. Biotechnol. 74 (1999) 337.

[67] V.K. Gupta, I. Ali, V.K. Saini, T. Van Gerven, B. Van der Bruggen, C. Vandecasteele, Ind. Eng. Chem. Res. 44 (10) (2005) 3655–3664.
[68] M. Ozacar, I.A. Sengil, J. Hazard. Mater. 98 (1–3) (2003) 211–224.
[69] I.D. Mall, V.C. Srivastava, N.K. Agarwal, Dyes Pigments 69 (2006) 210–223.
[70] Z. Al-qodah, Water Res. 34 (17) (2000) 4295–4303.
[71] G. McKay, H.S. Blair, J.R. Gardner, J. Colloid Interf. Sci. 95 (1983) 108.
[72] H. Nollet, M. Roels, P. Lutgen, P. Van der Meeren, W. Verstraete, Chemosphere 53 (2003) 655–665.
[73] M.S. Chiou, H.Y. Li, Chemosphere 50 (2003) 1095–1105.
[74] K.J. Laidler, J.M. Meiser, Physical Chemistry, Houghton Mifflin, New York, 1999, p. 852.
[75] M.J. Jaycock, G.D. Parfitt, Chemistry of Interfaces, Ellis Horwood Ltd., Onichester, 1981.
[76] D. Singh, Adsorp. Sci. Technol. 18 (8) (2000) 741–748.